

Linear radial growth velocity of isolated spherulites in polymer free solidification

Tao Huang*, A. D. Rey and M. R. Kamal†

Department of Chemical Engineering, McGill University, Montreal, Quebec, Canada
H3A 2A7

(Received 9 August 1993; revised 20 April 1994)

Real-time *in situ* observations of isolated spherulitic growth in poly(ethylene oxide) (PEO, $M_n = 100\,000$) and α -phase isotactic polypropylene (iPP, $M_n = 250\,000$) have been carried out by using video microscopy coupled with a computer image-processing system. A macroscopic latent heat transfer model, which is consistent with the linear growth velocity measured experimentally during spherulitic growth, has been developed and tested in conjunction with Hoffman's nucleation theory. It was found that the latent heat release during spherulitic solidification is compatible with the linear growth velocity.

(Keywords: polymer-free solidification; isolated spherulite; radial growth)

INTRODUCTION

A large variety of microstructures are obtainable during the solidification of most polymeric materials. Among these, spherulite growth is a frequently observed phenomenon in free solidification processing of all commercial semicrystalline polymers. Since the pioneering work on spherulitic polymer crystallization by Keith and Padden¹, much insight has been gained regarding the classification of morphologies and the associated lamellar structure². Although there are many reports relating to overall crystallization kinetics³, few details are available concerning spherulitic growth mechanisms and solidification kinetics. Hoffman and co-workers⁴ formulated a nucleation theory to describe the kinetics of polymer crystallization. They assumed that chain folding and lamellar formation are kinetically controlled, producing a metastable crystal. The concept of reptation was employed to account for chain mobility in the crystallization process, where the strong force resulting from the free energy difference between the subcooled melt and the lamellar crystal is envisaged to draw the chain through a reptation tube onto the crystal/melt interface.

In most published works, the spherulitic growth rate is determined from the position of the crystallization front in successive time intervals. The published growth size data show very good linearity. Recently, the precision of the measurements on spherulitic growth rate has been brought into question⁵. In polarized light microscopy many polymers show some roughness and coarseness of the crystallization front because the growth of crystals forming the front undergoes fluctuations, related to the fluctuations in secondary nucleation and in lamellar branching. The precision of the measurement is dependent on the sharpness and the optical contrast of

the crystallization front. As reported in ref. 5, spherulite growth rate measurements in various polymers often show significant discrepancies. Fluctuations around a mean growth rate value appear more clearly if the data are collected at shorter time intervals. In order to re-examine the linearity of spherulitic growth rate, a technique is needed that would permit high-precision determination of spherulitic growth rates and to measure the growth rate under isothermal conditions.

It is often assumed that polymer crystallization involves no temperature gradient across the melt–solid interface. However, this assumption is not valid because polymers usually crystallize significantly below the melting point. The temperature at the crystallization front may be well below the equilibrium melting point but above the temperature of the supercooled melt phase. The heat conduction problem associated with the above description has not been dealt with in detail, especially for the case associated with constant spherulitic growth rate during solidification. This problem has been considered recently⁶, assuming an infinite planar crystallization front. The computational results indicated that the temperature rise at the interface may reach 50–60°C at infinite times. However, it was pointed out⁶ that, for most polymers, the temperature increase is only a fraction of a degree in a reasonable experimental time-scale (minutes or hours).

In the present work, an experimental technique for high-precision determination and measurement of the spherulitic growth rates has been developed. The technique employs video microscopy, coupled with a computer image-processing system. Real-time *in situ* observations of isolated spherulitic growth in poly(ethylene oxide) (PEO, $M_n = 100\,000$) and α -phase isotactic polypropylene (iPP, $M_n = 250\,000$) have been carried out to confirm the linearity of the spherulitic growth rate. A macroscopic latent-heat transfer model has been developed and tested in conjunction with Hoffman's nucleation equation. The results are consistent with the linear growth velocity measured experimentally during spherulitic growth.

* Permanent address: Department of Materials Science and Engineering, Northwestern Polytechnical University, Xi'an 710072, People's Republic of China

† To whom correspondence should be addressed

Table 1 Selected properties of PEO and iPP

	PEO	iPP
Molecular weight ^a	100 000 (M_n)	250 000 (M_n)
Equilibrium melting point, T_m (K)	341.7 ¹⁰	458.2 ¹¹
Heat of fusion, L (kJ mol ⁻¹)	8.31 ¹⁸	8.79 ¹⁸
Specific heat of melt ^b C_p (J mol ⁻¹ K ⁻¹)	95 ²⁰	101.96 ²¹
Thermal diffusivity ^c , a (cm ² s ⁻¹)	9.0 × 10 ⁻⁴	6.48 × 10 ⁻⁴
	(ref. 22)	(ref. 23)
Glass transition temperature T_g (K)	196	269.6
Diffusional activation energy Q (kJ mol ⁻¹)	29.7 ¹⁰	6.28 ¹¹

^a Supplied by Aldrich Chemical Company Inc.

^b C_p for PEO melt at 340 K and iPP melt at 400 K

^c a for PEO melt at 340 K and iPP melt at 400 K

EXPERIMENTAL

Materials and properties

Experiments were carried out with poly(ethylene oxide) (PEO, $M_n = 100\,000$) and α -phase isotactic polypropylene (iPP, $M_n = 250\,000$), both supplied by Aldrich Chemical Company Inc. (Aldrich catalogue no. 18 198-6 for PEO and 18 238-9 for iPP, respectively). Table 1 gives the relevant physical properties of the PEO and iPP used in this study. The polydispersity M_w/M_n for the PEO is estimated to be below 1.1. It is estimated that for the iPP employed in this study, M_w/M_n is around 2.3–2.5 (ref. 7). There are many studies relating to low-molecular-mass PEO fractions ($M_w = 2000$ – $10\,000$), which have led to a basic understanding of the melt crystallization behaviour of this polymer⁸. Recently, chain folding characteristics and the change in crystal morphologies of these low-molecular-weight PEO single crystal growth systems have been established over a wide range of supercooling ($\Delta T = 20^\circ\text{C}$) by Cheng *et al.*⁹. Cheng *et al.*^{10–12} reported experimental results regarding crystal growth of intermediate molecular mass PEO fractions ($M_w = 23\,000$ – $105\,000$) from the melt and examined the linear crystal growth rates and crystalline morphology changes in a set of polypropylene fractions with similar molecular masses and distributions but different isotacticities. Other recent studies evaluated the overall crystallization kinetics of iPP–diluent and iPP blend systems^{13–15}.

The present study concentrates on the selection of radial growth velocity and the evolution of spherulitic pattern in order to obtain a phenomenological explanation of these aspects. Crystallization temperatures in the range $T_0 = 45$ – 54°C for PEO and $T_0 = 120$ – 142°C for the α -phase iPP have been employed. The above ranges were chosen to avoid the multiple morphologies which exist in PEO crystallization and the multiple crystalline forms for iPP. Thus, the current effect does not deal with the growth regime transition phenomenon^{4,9–11}.

Sample preparation

PEO fractions were dried in a vacuum oven to remove gas and bubbles that were absorbed or dissolved in the polymer powder. Melting and resolidification treatments were applied to the sample prior to any measurements and experiments. About 1–2 mg of PEO or iPP were melted on a glass slide (25 × 25 mm) in a vacuum oven. Then, a polymer film was formed by covering with the top glass slide and pressing the top slide to form a 10 μm

thick polymer film. The thickness is controlled by an aluminium film spacer placed between the glass slides. In order to avoid changes in the thickness of the specimen as well as evaporation during melting or sublimation of solids in the polymer sample and to reduce the possibility of degradation, a carefully selected adhesive seals the specimen.

In situ observation system for isolated spherulite growth

A Leitz Polarizing Microscope (Laborlux 12 Pol S), equipped with a Leitz Heating Stage 350/Digital basic unit and a 35 mm camera or JAVELIN electronic Chromachip II MOS Sensor Colour Camera (JE3462HR), was used in this study. The preset temperatures of the heating stage can be kept constant to $\pm 0.1^\circ\text{C}$, and heating or cooling rates of up to $20^\circ\text{C min}^{-1}$ are possible. Temperature measurements were carried out by inserting a very fine (5 μm in diameter) thermocouple in the sample.

In order to make the observations and measurements automatically and with high accuracy, JAVA-Jandel Scientific's video measurement and analysis software with PCVISIONplus hardware system, was directly connected to the PLM microscope via the CCD camera. This image-processing system made it possible to capture an image of the growing spherulite, enhance it as necessary, make a series of measurements and then analyse and output both data and images. The video pictures are digitized into 512×480 pixel images of 256 grey values and stored in the computer memory. The resolution is not limited by the periscope. The resulting magnification of the pixel between 0.97 and 1.36 $\mu\text{m/pixel}$ is limited by the total number of pixels of the frame buffer as a result of compromise between the size of the object plane and the magnification of the pictures. The distortion in linear measurement is less than 1%.

Measurement of growth velocity and characteristic size of the spherulite

In order to observe the growth of an isolated spherulite successfully, the nucleation density in a given unit area should be as low as possible. The nucleation density is influenced by two factors: the melting temperature and the holding time at this melting temperature. The density decreases with increasing melting temperature and holding time, because these two factors affect the self-seeded nuclei and reduce the memory effects of the former microstructure. Heat treatment was at 75°C for 10 min for PEO and at 190°C for 20 min for iPP in the present studies. Subsequently, the specimen was quenched quickly in the oven of the heating stage to the preset free solidification temperature.

In order to enhance the sharpness of the crystallization front, transmitted light was used to capture the envelope of a growing spherulite. Computer image enhancement processing was used to remove the influence of the birefringence due to polarized light on the determination of the overall crystallization front. In order to obtain the precise interface location, instead of measuring the increase of the radius which was used in most of the published reports, the growth velocity is determined by using the computer image-processing system to measure the area within the envelope of the spherulite¹⁵,

$$V = \frac{ds}{dt} \frac{1}{2\sqrt{\pi s}} \quad (1)$$

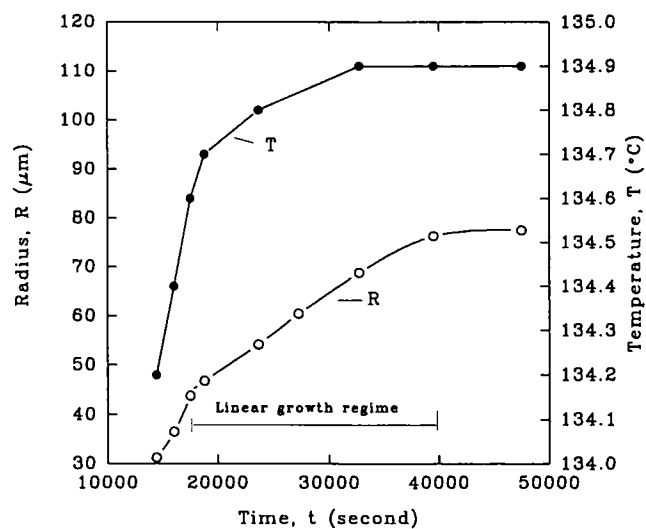


Figure 1 Typical variation of the size of a growing iPP spherulite with time and the corresponding increase in temperature during growth; $T_0 = 134.0^\circ\text{C}$

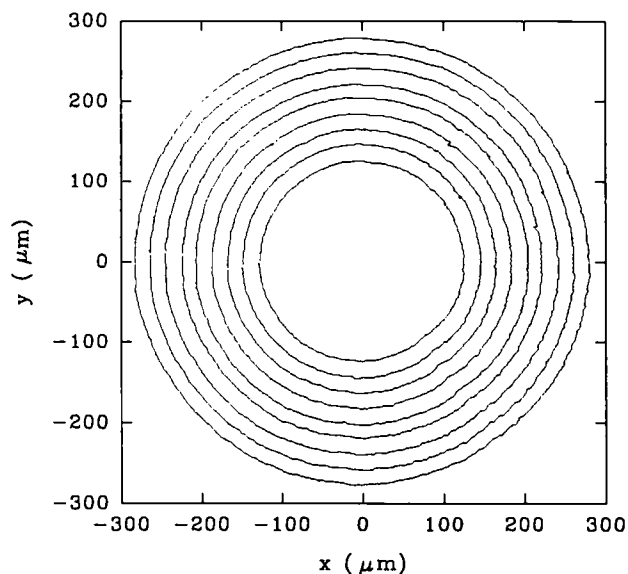


Figure 2 The iso-contours of PEO spherulite extracted at the time intervals (s): 0 (time to count); 2.49; 4.39; 6.36; 8.68; 10.66; 12.65; 14.73; 16.71. $T_0 = 46.6^\circ\text{C}$

where V is spherulitic growth rate, t is time and s is the measured projected area of the spherulite. The images were captured in shorter time intervals (5 s for PEO during 300 s growth times, and 1000 s for iPP during 24 h growth times for an isolated spherulite). The precision of the measurement of time intervals was better than 0.1 s.

Data on both areas and radii are transformed automatically by the computer. The accuracy of measurements of average interface velocities is of the order of $10^{-5} \mu\text{m s}^{-1}$. Figure 1 presents a typical curve of the evolution of the size of a growing spherulite with time and the increase in temperature during the growth. It indicates that the overall growth process of a spherulite consists of three stages: the evolution of spherulitic growth ranging from a folded-chain single crystal to a fully developed spherulite, the stable growth of the spherulite with a linear behaviour, and the non-linear growth stage due to impingement. The present study will focus on the linear growth of the stable state.

RESULTS

The detection of the interface of the spherulite is performed on the enhanced transmission light image by the image-processing software. Figure 2 shows iso-contours of the PEO spherulite extracted at different time intervals. It shows that the spatial evolution of the spherulite envelope is fairly well distributed and increases linearly. The results of video image measurements confirm the linear radial growth velocity, as shown in Figure 3. Figure 4 shows the dependence of linear radial growth velocity on temperature. These results are in agreement with data reported by Cheng and co-workers¹⁰. Figure 5 shows iso-contours of the iPP spherulite extracted at different time intervals. It shows that there is some oscillation in the spatial evolution of the iPP spherulite envelope. The results of video image analysis still confirm the linear radial growth velocity, as shown in Figure 6. Figure 7 shows the dependence of linear radial growth velocity on temperature.

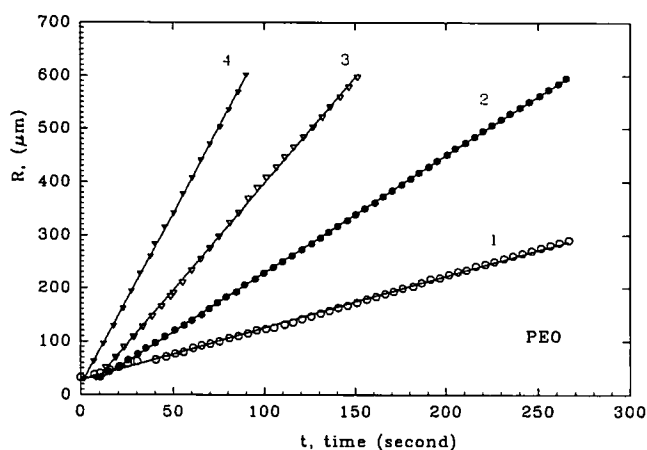


Figure 3 Graph showing linear radial growth of PEO spherulites at different temperatures. 1, $T_0 = 52.6^\circ\text{C}$, $V = 0.793 \mu\text{m s}^{-1}$; 2, $T_0 = 51^\circ\text{C}$, $V = 2.231 \mu\text{m s}^{-1}$; 3, $T_0 = 49.5^\circ\text{C}$, $V = 3.79 \mu\text{m s}^{-1}$; 4, $T_0 = 46.6^\circ\text{C}$, $V = 6.668 \mu\text{m s}^{-1}$

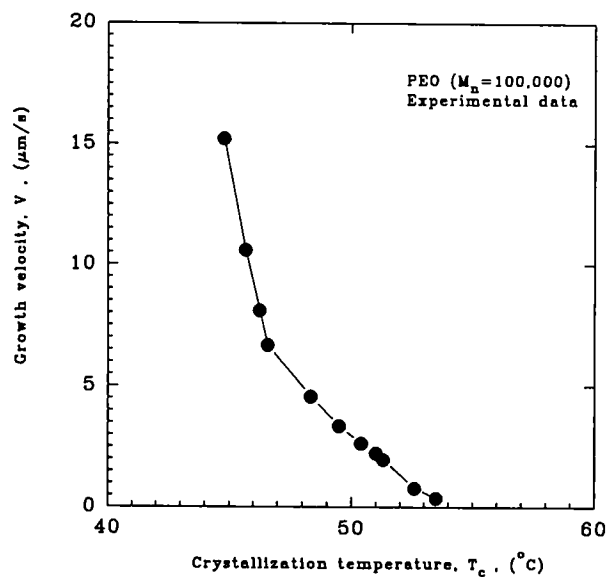


Figure 4 PEO spherulite growth velocities at different temperatures. The line is through the experimental data, not theoretical prediction

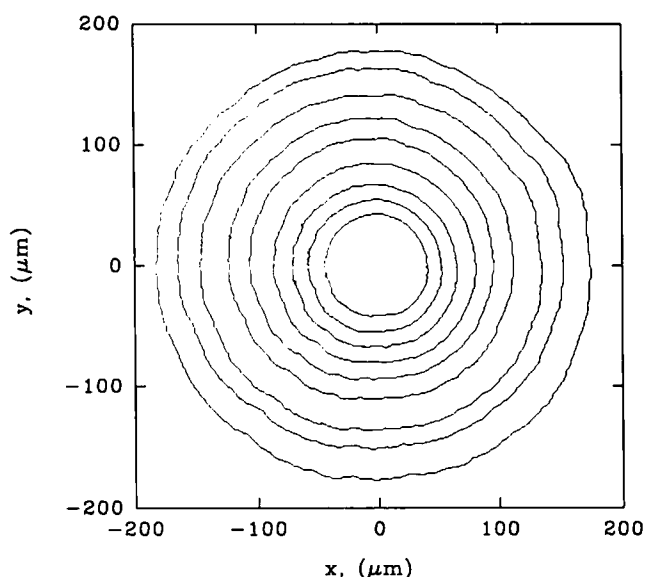


Figure 5 The iso-contours of iPP spherulite extracted at the time intervals (min): 0 (time to count); 31; 61; 92; 123; 172; 195; 244. $T_0 = 140^\circ\text{C}$

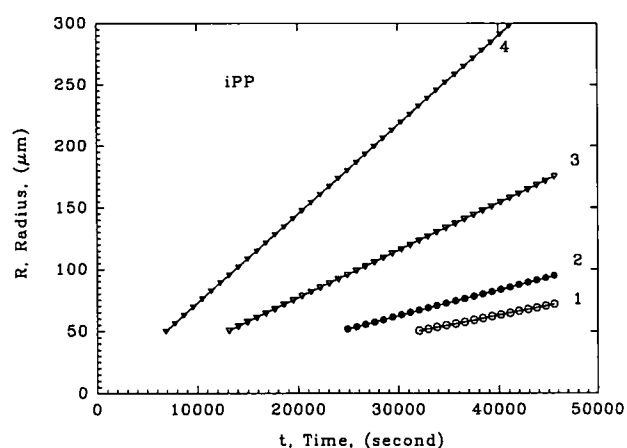


Figure 6 Graph showing linear radial growth of iPP spherulites at different temperatures. 1, $T_0 = 141^\circ\text{C}$, $V = 0.0157 \mu\text{m s}^{-1}$; 2, $T_0 = 136^\circ\text{C}$, $V = 0.02 \mu\text{m s}^{-1}$; 3, $T_0 = 130^\circ\text{C}$, $V = 0.0725 \mu\text{m s}^{-1}$; 4, $T_0 = 128^\circ\text{C}$, $V = 0.1225 \mu\text{m s}^{-1}$

DISCUSSION

The shapes of growing crystallizing solids are determined by an interplay of complex processes that include transport of energy and matter through bulk phases, capillarity-related processes that determine local equilibrium conditions at the solid-melt interface, and non-equilibrium kinetic processes that take place locally at that interface. The mathematical description of solidification results in free boundary problems, which are quite difficult to solve.

The solidification process in polymers involves a moving solid/melt front. This front consists of a lamellar crystalline phase and an amorphous phase. The liberation of the latent heat at the interface must be conducted away from the moving front. Crystal growth of the lamellar crystalline phase in a homopolymer from the melt is generally accompanied by segregation and resulting redistribution of molecular species. The diffusivity of each chain molecule in a polymer melt is strongly dependent on its individual length, i.e. upon its individual molecular

weight. Although concentration profiles are significantly altered with broad distributions of molecular weight, and long segregated molecules dominate morphologically important behaviour, the influence of reptation upon concentration profiles is slight when segregated species have relatively narrow distributions of molecular weight¹⁶. The reptation effect can be considered together with the growth in non-equilibrium interfacial kinetics, as shown in the following section. On the other hand, results reported by Cheng *et al.*⁹⁻¹² on a set of mass fractions of PEO and iPP show that molecular weight polydispersity and isotacticity do not affect the linearity of growth rate.

Because polymers usually crystallize at temperatures well below the melting point and the formed solids are far removed from equilibrium, the temperature of the growth front should be well below the equilibrium melting point but above the preset temperature of the supercooled melt in the bulk. Hence, the solidification of polymers is a special case, and an isothermal pure 'solute' model of isothermal solidification would not be viable. One should consider the influence of the effects of latent heat conduction.

Non-equilibrium interfacial kinetics effects

It is generally accepted that for crystal growth behaviour, the rate-limiting steps may be either the rate of diffusion of molecules to or from the growth surface (diffusion control) or the rate of attachment of such molecules to the interface once they arrived (interface control). For diffusion control, $R = C_1 t^{1/2}$ where R is the radius and C_1 is a constant. If the growth process is interface controlled, the linear growth rate is constant with time, since molecules are always present at the surface and surface sites are filled at a constant frequency, thus $R = Vt$ where $V = \text{constant}$. Our experiments clearly show that the spherulitic solidification for both PEO and iPP was interface controlled, that is, $R = Vt$ where $V = \text{constant}$.

The growth velocity V of polymer crystals determined by surface nucleation and macromolecular reptation is

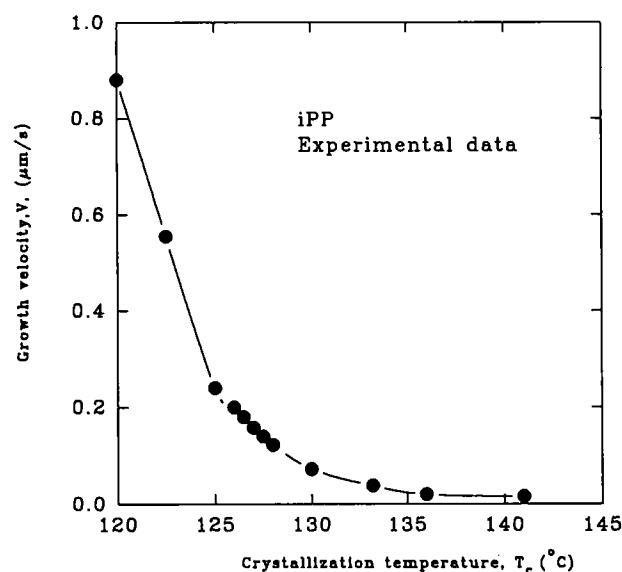


Figure 7 iPP spherulite growth velocities at different temperatures. The line is drawn through the experimental data, not theoretical prediction

described by the following equation⁴:

$$V = V_0(\Delta T) \exp\left[\frac{-Q}{R_0(T_c - T_x)}\right] \exp\left(\frac{-K_g}{T_c(\Delta T)f}\right) \quad (2)$$

where V_0 and K_g are constants, Q is the diffusional activation energy, $R_0 = 8.314 \text{ J mol}^{-1} \text{ K}^{-1}$ is the gas constant, and $T_x = T_g - 30 \text{ K}$, T_g is the glass transition temperature. $\Delta T = T_m - T_c$ is the supercooling and $f = 2T_c/(T_m + T_c)$, where T_m is the equilibrium melting point and T_c is a preset crystallization temperature.

Thermal conduction and latent heat effects on spherulitic growth

As a classical Stefan moving boundary problem, the heat conduction-limited velocity for a uniform, smooth, spherical growth front is usually considered to follow a square-root relation as follows:

$$V = \lambda_T(a/t)^{1/2} \quad (3)$$

where a is a constant and λ_T is a growth coefficient. The expression for heat rejection, in this case, is given by the well known equation¹⁷:

$$2\lambda_T^2 - 2\sqrt{\pi}\lambda_T^3 \exp(\lambda_T^2) \operatorname{erfc}(\lambda_T) = \Delta T/(L/C_p) \quad (4)$$

where ΔT is supercooling, L is the heat of fusion and C_p is the specific heat. The predicted heat conduction-limited growth velocities according to equation (4) versus the instantaneous radii of the corresponding spherulites, do not agree with experimental measurements, as expected.

Recently, Piorkowska and Galeski⁶ considered the influence of the liberation of heat of fusion on the temperature near the crystallization front in polymers with a model of an infinite, planar surface of solidification moving with constant speed. In this case, the temperature of the growth front is given by

$$T_i(0, t) = T_c + [s_c L d_c / d_a C_p] \operatorname{erf}(V\sqrt{t}/2\sqrt{a}) \quad (5)$$

where C_p denotes the specific heat capacity of the medium, d_a and d_c denote the density of the amorphous phase and the density of the crystalline phase, respectively, s_c is the degree of crystallinity of the spherulite, and L is the latent heat. This model suggests that a constant crystalline phase growth rate gives a continuously increasing temperature at the crystallization front and the surroundings. For an infinite time of crystallization, the temperature rise may reach 50–60°C⁶. However, the experimental results in Figure 1 reported in the present work have shown that the temperature increase is only a fraction of a degree in a reasonable time-scale (minutes or hours).

Proposed model

For unperturbed growth of the spherulitic envelope, in a radial coordinate system, all the quantities depend only on radius r and time t . For reasons of symmetry, the unperturbed growth of the spherulitic envelope is essentially one-dimensional in space. Let us consider two of the coordinate frames: one is the fixed frame, with the origin fixed at the centre of the spherulite, and the other is the moving front of the spherulite envelope located at $r = R(t)$ in the fixed frame. In the moving frame, the thermal conduction equation is:

$$\frac{\partial T}{\partial t} = a \left[\frac{\partial^2 T}{\partial r^2} + \frac{2}{R(t)+r} \frac{\partial T}{\partial r} \right] + \frac{dR}{dt} \frac{\partial T}{\partial r} \quad (6)$$

The following boundary conditions are employed:

(i) Linear growth velocity (assumed on the basis of experimental results):

$$dR/dt = V = \text{constant} \quad (7)$$

(ii) The isothermal crystallization temperature, T_c , is obtained far from the moving front:

$$T(\infty, t) = T_c \quad (8)$$

When the heat is generated at the melt/solid front, the conduction of heat must be shared by the supercooled melt and the growing solid. The heat flow into the solid results in the temperature rise of the spherulite solid. In the present work, the temperature everywhere inside the spherulite solid is assumed to be equal to the interface temperature T_i . The model employed in this work is the so-called 'one-sided' model, which is widely used in crystal growth work¹⁸. It works well for polymer solidification for various reasons: (a) the size of the isolated spherulite compared with the surrounding melt is quite small; (b) the spherulite grows well below the equilibrium melting point; and (c) the differences between the thermal diffusivities and specific heats of the melt and the semicrystalline polymer solid are small at the crystallization temperatures, e.g. for iPP, specific heat at $T = 410 \text{ K}$, $C_p^s = 102.20 \text{ J K}^{-1} \text{ mol}^{-1}$, $C_p^l = 104.99 \text{ J K}^{-1} \text{ mol}^{-1}$ (ref. 21); the thermal diffusivity of iPP is 6.4×10^{-4} and $6.6 \times 10^{-4} \text{ cm}^2 \text{ s}^{-1}$ at temperatures $T = 353.2 \text{ K}$ and $T = 463.2 \text{ K}$, respectively²².

(iii) The temperature gradient at the solid/melt interface ($r = 0$):

$$(\partial T / \partial r) = -L\beta / C_p \quad (9)$$

where $\beta = V/a$. This equation indicates the relation between the heat production due to the volume change, as a result of crystallization, and the shift of the temperature throughout the solid.

The solution of equation (6) is given below:

$$T(R+r) - T_c = \frac{L}{C_p} \beta R^2 \left[\frac{\exp(-\beta r)}{R+r} + \beta \exp(\beta R) \operatorname{Ei}[-\beta(R+r)] \right] \quad (10)$$

where $\operatorname{Ei}(p)$ is the exponential integral function

$$\operatorname{Ei}(p) = \int_p^\infty \frac{\exp(-x)}{x} dx \quad (11)$$

and its series expansion is

$$\operatorname{Ei}(p) = -\gamma - \ln p - \sum \frac{(-1)^n p^n}{n!} \quad (12)$$

where $n = 1, 2, \dots, \infty$ and $\gamma = 0.5772156649 \dots$ is Euler's constant.

At the interface $r = 0$, the interface temperature is given by:

$$T_i = T_c + (L/C_p)\beta R [1 + \beta R \exp(\beta R) \operatorname{Ei}[-\beta R]] \quad (13)$$

and the temperature rise is

$$\Delta T_i = T_i - T_c = \frac{L}{C_p} \frac{VR}{a} \left[1 + \frac{VR}{a} \exp\left(\frac{VR}{a}\right) \operatorname{Ei}\left(-\frac{VR}{a}\right) \right] \quad (14)$$

Under the experimental conditions employed in this study, for PEO, the growth velocity is in the range $0.1\text{--}20 \mu\text{m s}^{-1}$ and the growth time $t < 50 \text{ s}$. The numerical

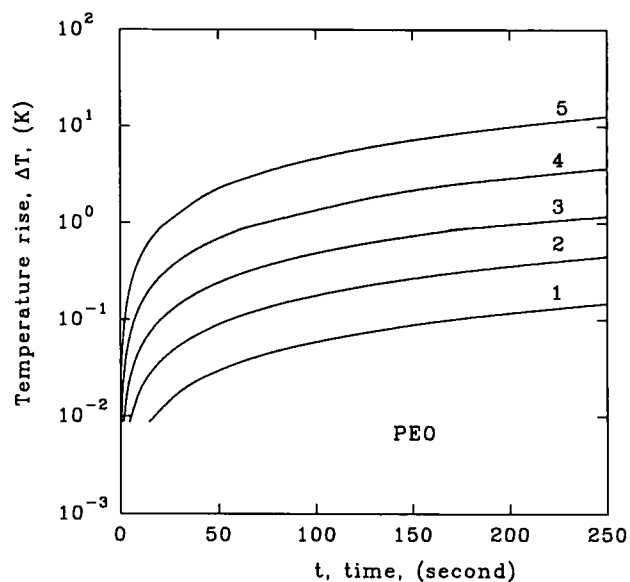


Figure 8 The calculated results for increased interface temperature ΔT with time t for PEO. 1, $V=0.793 \mu\text{m s}^{-1}$; 2, $V=1.3785 \mu\text{m s}^{-1}$; 3, $V=2.264 \mu\text{m s}^{-1}$; 4, $V=3.79 \mu\text{m s}^{-1}$; 5, $V=6.668 \mu\text{m s}^{-1}$

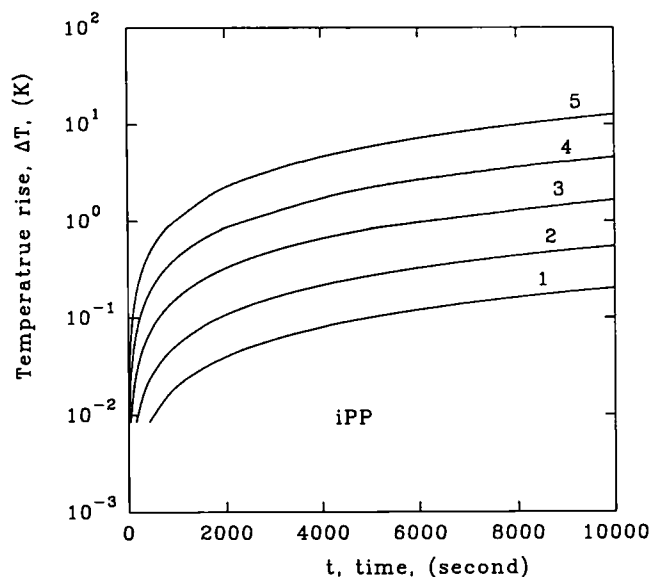


Figure 9 The calculated results for increased interface temperature ΔT with time t for iPP. 1, $V=0.0236 \mu\text{m s}^{-1}$; 2, $V=0.0385 \mu\text{m s}^{-1}$; 3, $V=0.0725 \mu\text{m s}^{-1}$; 4, $V=0.14 \mu\text{m s}^{-1}$; 5, $V=0.24 \mu\text{m s}^{-1}$

results calculated from equation (14) are shown in Figure 8. These results indicate that the increased interface temperature is less than 1°C . For iPP, the growth velocity is in the range $0.01\text{--}0.1 \mu\text{m s}^{-1}$ and the growth time-scale is 10^4 s. The calculated results, using equation (14), show that the increase in interface temperature is of the order of 1°C , as shown in Figure 9. This is in quantitative agreement with the experimental observations and measurements given in Figure 1. Figure 10 and Figure 11 show plots based on experimental data of $(\log V - \log(T_m - T_c) + Q/2.303R_0(T_c - T_g + 30))$ versus $(1/T_c(T_m - T_c)f)$ for PEO and iPP, respectively, where $f = 2T_c/(T_c + T_m)$. It is seen that the experimental data follow a straight line. Thus, the effect of latent heat release is relatively smaller. Obviously, this behaviour depends on the thermophysical properties of the polymer.

CONCLUSION

Video measurement and a computer image analysis system were used to capture the velocities and interfacial pattern of PEO and iPP polymeric spherulitic growth fronts. Experimental results confirmed the growth rate linearity. A phenomenological explanation is proposed for the selection of radial growth velocity and the evolution of the spherulitic pattern. A hybrid model is presented combining the latent heat release model with Hoffman's nucleation theory. The model produces predictions of spherulitic growth velocity in agreement with experimental results. This model confirms that latent heat release during spherulitic solidification is compatible with the linear growth velocity.

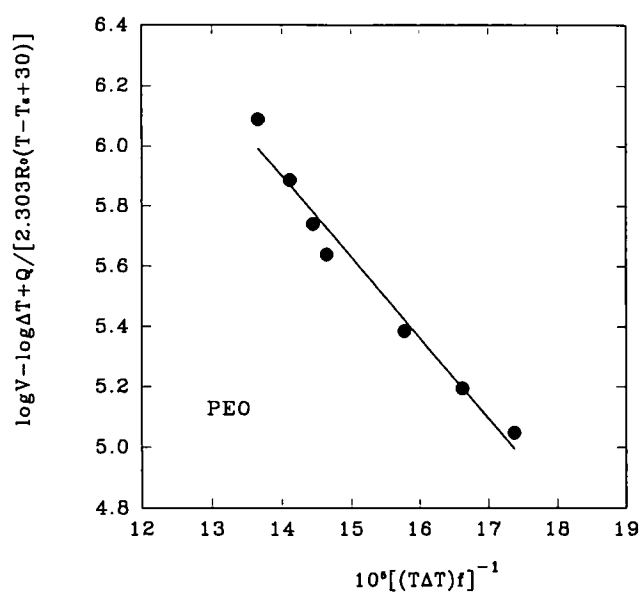


Figure 10 The kinetics law for studied PEO spherulitic growth

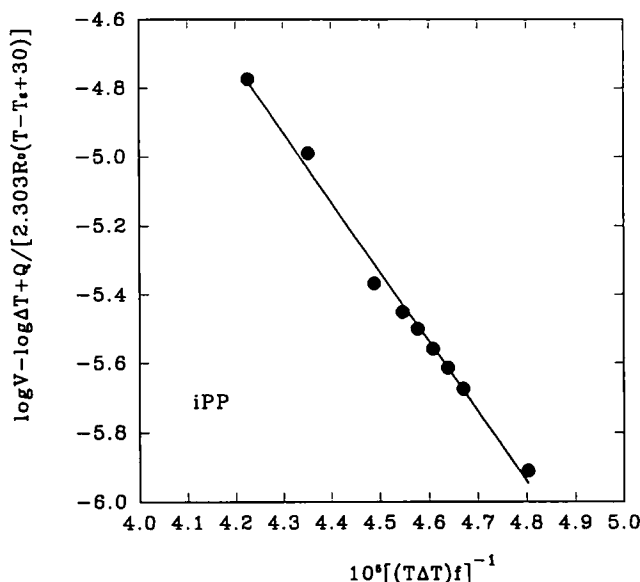


Figure 11 The kinetics law for studied iPP spherulitic growth

ACKNOWLEDGEMENTS

One of us (T.H.) is grateful to the Aerospace Administration of People's Republic of China for partial support during his stay at McGill University. The authors would like to acknowledge financial support from the Natural Science and Engineering Research Council of Canada and Ministère de l'Éducation, Gouvernement du Québec.

REFERENCES

- 1 Keith, H. D. and Padden, F. J. Jr. *J. Appl. Phys.* 1963, **34**, 2409; 1964, **35**, 1270, 1286
- 2 Phillips, P. J. *Rep. Prog. Phys.* 1990, **53**, 549
- 3 Eder, G., Janeschitz-Kriegl, H. and Liedauer, S. *Prog. Polym. Sci.* 1990, **15**, 629
- 4 Hoffman, J. D. and Miller, R. L. *Macromolecules* 1988, **21**, 3038
- 5 Pawlak, A. and Galeski, A. *J. Polym. Sci., Phys. Edn* 1990, **28**, 1813
- 6 Piorkowski, E. and Galeski, A. *Polymer* 1992, **33**, 3985
- 7 Bohossian, T. and Delmas, G. *J. Polym. Sci., Phys. Edn* 1992, **30**, 993
- 8 Kovacs, A. J. and Straupe, C. *J. Cryst. Growth* 1980, **48**, 210
- 9 Cheng, S. Z. D., Zhang, A., Chen, J. and Heberer, D. P. *J. Polym. Sci., Phys. Edn* 1990, **29**, 311
- 10 Cheng, S. Z. D., Chen, J. and Janimak, J. J. *Polymer* 1990, **31**, 1018
- 11 Cheng, S. Z. D., Janimak, J. J., Zhang, A. and Chang, H. N. *Macromolecules* 1990, **23**, 298
- 12 Janimak, J. J., Cheng, S. Z. D. and Giusti, P. A. *Macromolecules* 1991, **24**, 2253
- 13 Lim, G. B. A. and Lloyd, D. R. *Polym. Eng. Sci.* 1993, **33**, 513, 522, 529, 537
- 14 Wang, Y. F. and Lloyd, D. R. *Polymer* 1993, **34**, 2324
- 15 Long, Y., Stachurski, Z. H. and Shanks, R. A. *Mater. Forum* 1992, **16**, 259
- 16 Keith, H. D. and Padden, F. J. Jr. *J. Polym. Sci., Phys. Edn.* 1987, **25**, 229, 2265
- 17 Carslaw, H. S. and Jaeger, J. C. 'Conduction of Heat in Solids', Oxford University Press, London, 1959, Ch. XI
- 18 Langer, J. S. *Rev. Mod. Phys.* 1980, **52**, 1
- 19 Brandrup, J. and Immergut, E. H. 'Polymer Handbook', John Wiley, New York, 1989
- 20 Van Krevelen, D. W. 'Properties of Polymers', Elsevier, Amsterdam, 1990
- 21 Gaur, U. and Wunderlich, B. *J. Phys. Chem. Ref. Data* 1981, **10**, 1051
- 22 Askadskii, A. A. in 'Encyclopedia of Flow Mechanics', Gulf Publishing Company, Houston, TX, 1989, vol. 19, p. 103
- 23 Touloukian, Y. S. 'Thermal Diffusivity', IFI, Plenum, New York, 1973